Postsynthetic Modification Strengthens the Stereoselectively Self-Assembled Hemiaminal Ether Complexes

*Sakthi Raje, Mahesh Sundararajan and Raja Angamuthu**

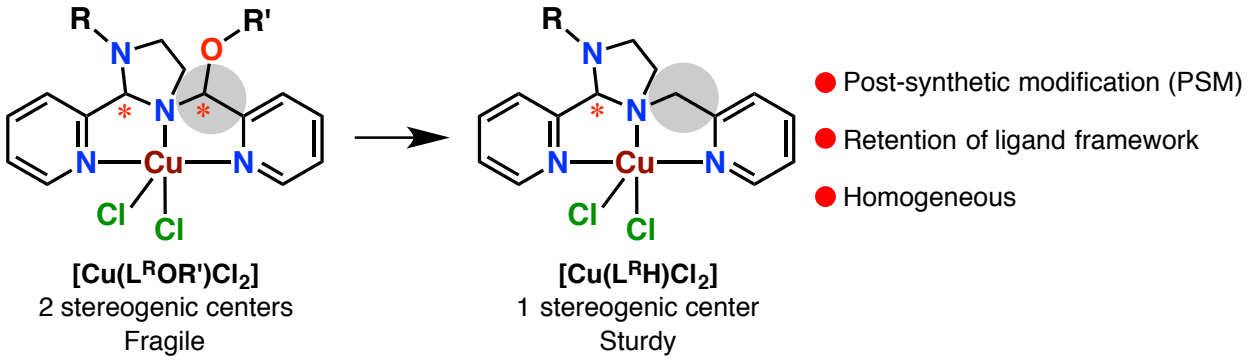

ABSTRACT. Fragile hemiaminal ether linkages present in the backbone of koneramines (L^ROR'), potential tridentate ligands, bound to copper(II) in stereoselectively self-assembled *syn*-[$Cu(L^ROR')X_2$] complexes were transformed into sturdy methylene linkages to make corresponding *rac*-[$Cu(L^RH)Cl_2$] complexes by homogeneous postsynthetic modification with the retention of coordination sphere. The generality of stereoselective self-assembly of koneramine complexes is shown by utilising a number of metal ions, anions, amines, alcohols and thiols with complete characterisations.

INTRODUCTION. Postsynthetic modification (PSM) of molecular architectures is an important and interesting concept in the context of late-stage modifications,[1-4] tweaking solubility[4, 5] and diverting equilibrium reactions towards the formation of a desired one among many possible molecules.[6] As Seth Cohen stated "PSM involves the chemical modification of a coordination network in a heterogeneous fashion on the already-formed solid network by an external reagent that is present in the solution or gas phase. Retention of structure and crystallinity with respect to the original material is an essential feature of most useful PSM reactions".[7] Small or mononuclear molecules might not be as compatible towards PSM as larger systems, metal-organic frameworks (MOFs), covalent organic frameworks (COFs) and polymers[6, 8-12] owing to the pronounced structural integrity provided by the stable (supramolecular) architecture present in MOFs and COFs.[13]

Our one-pot protocol allowed the stereoselective (syn or anti) and geometry specific (facial or meridional) assembly of hemiaminal ether ligands (L^ROR') comprising 2,2'-dipicolylamine backbone in good yield from prebiotically relevant multicomponent pool of mono-*N*-substituted ethylenediamines, pyridine-2-carboxaldehyde and primary alcohols or thiols

at ambient conditions.[14-17] Although the multicomponent mixture contained both *syn* (RR and SS) and *anti* (RS and SR) forms of hemiaminal ether L^{R}OR' is in dynamic equilibrium with plethora of other components such as hemiaminal and imidazoline, we succeeded to trap *syn*-L^{R}OR' as complexes with Cu(II) and Zn(II) ions and *anti*-L^{R}OR' by employing Ni(II) and Cd(II) ions. Hemiaminal or hemiaminal ether moieties are known to be Achilles' heel and seldom isolated as part of cyclic compounds.[18, 19]

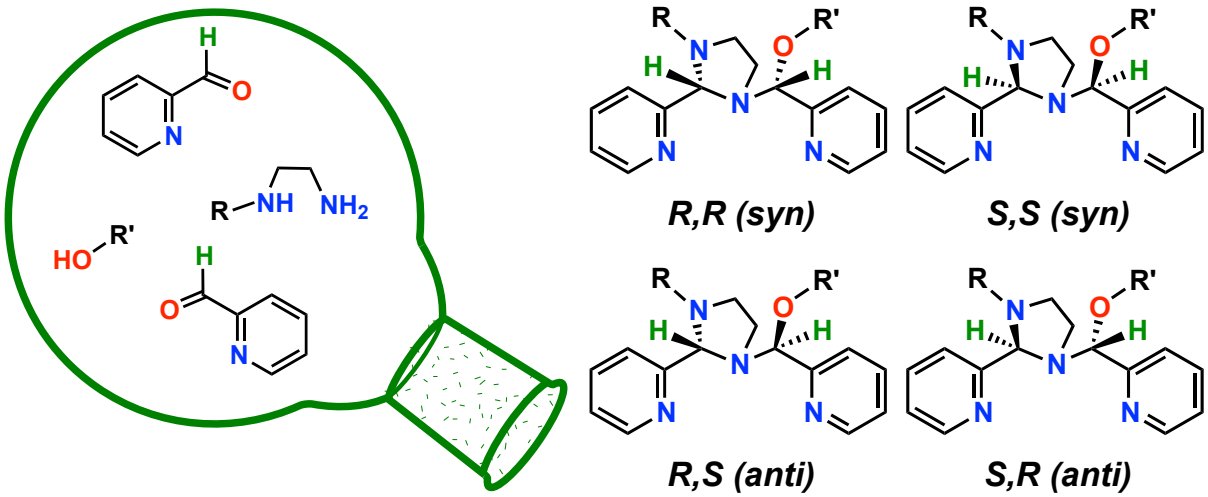

Fig. 1. Assembly of koneramines (L^{R}OR') and the possible stereoisomers. Cu(II) and Zn(II) trapped *syn*-koneramine, and Ni(II) and Cd(II) trapped in *anti*-koneramine diastereoselectively (R = Ph, Py, Et or Ts and R' = Me, Et, Pr or Bu).[14-17]

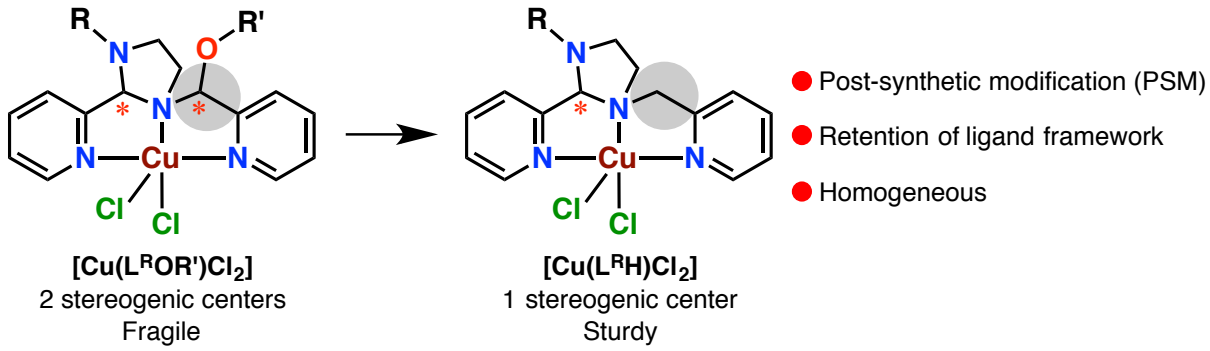

Fig. 2. Post-synthetic modification (PSM) of hemiaminal ether ligand (koneramine) coordinated to a Cu(II) ion.

Herein, we demonstrate that our protocol for stereoselective (syn or anti) and geometry specific (facial or meridional) assembly of hemiaminal ethers ($L^{R}OR'$) assembled through an emergent phenomenon is general and versatile, by changing every component of the prebiotically relevant multicomponent pool of aldehyde, amine and alcohol (Fig. 1). Furthermore we report the post-assembly modification of the fragile hemiaminal ether linkages (>N-C(H)(OMe)- Py) present in the backbone of koneramines ($L^{R}OR'$) bound to copper in *syn*-$[Cu(L^{R}OR')X_2]$ into stronger methylene linkages (>N-CH_2-Py) in addition to the decoordination and utilization of $L^{Ph}H$.

RESULTS AND DISCUSSION. In order to see the effect of alcoholic solvents in the formation of koneramines, a number of $[Cu(L^{Ph}OR')Cl_2]$ complexes were assembled successfully from 1:2 mixtures of *N*-phenylethylenediamine and pyridine-2-carboxaldehyde in corresponding alcohols (R' = Me,[14] Et, n-Pr, n-Bu and ^{i}Pr[16]; Fig. 3; Fig. S1-S9, ESI†). Previously, the complexes $[Zn(L^{Ph}OR')Cl_2]$ (R' = Me, Et, n-Pr, n-Bu) were also reported by us.[14] Ethyl mercaptan and 2-mercaptoethanol were used as nucleophilic solvents to isolate the complexes $[M(L^{Ph}SEt)Cl_2]$ (M is Cu, Zn) and $[M(L^{Ph}S(CH_2)_2OH)Cl_2]$ (M is Zn, Cd).[14, 15] However, when tert-BuOH was used, due to the steric bulk we have obtained the hemiaminal complex, $[Cu(L^{Ph}OH)Cl_2]$ instead of expected HAE complex $[Cu(L^{Ph}O^{t}Bu)Cl_2]$.[16] The formation of aforementioned complexes indicated that the HAE formation works in any primary and secondary alcohols and thiols except tertiary alcohols.

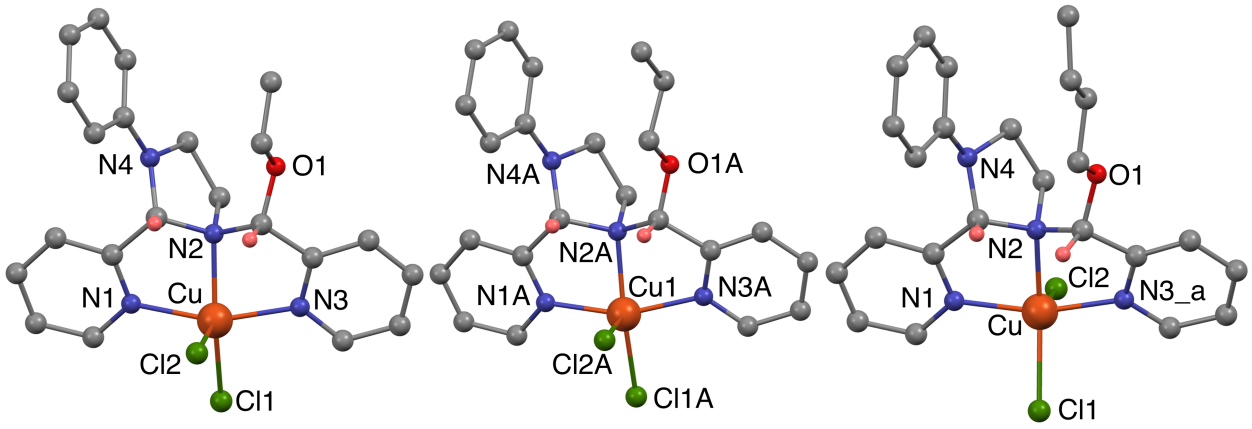

Fig 3. Solid-state structures of *syn*-[Cu(L^{Ph}OEt)Cl_2] (left), *syn*-[Cu(L^{Ph}OPr)Cl_2] (middle) and *syn*-[Cu(L^{Ph}OBu)Cl_2] (right). Solvents and H atoms other than those bound to the stereogenic centers are omitted for clarity. Selected bond distances (Å) and angles (°) *syn*-[Cu(L^{Ph}OEt)Cl_2]: Cu-N(3), 2.022(3); Cu-N(1), 2.027(3); Cu-N(2), 2.066(3); Cu-Cl(1), 2.2405(11); Cu-Cl(2), 2.5029(11); N(3)-Cu-N(1), 159.68(14) = β; N(3)-Cu-N(2), 80.69(13); N(1)-Cu-N(2), 80.26(13); N(3)-Cu-Cl(1), 97.47(10); N(1)-Cu-Cl(1), 97.66(10); N(2)-Cu-Cl(1), 158.54(10) = α; N(3)-Cu-Cl(2), 95.84(10); N(1)-Cu-Cl(2), 93.30(10); N(2)-Cu-Cl(2), 96.60(10); Cl(1)-Cu-Cl(2), 104.85(4). For *syn*-[Cu(L^{Ph}OPr)Cl_2]: Cu(1)-N(1A), 2.005(5); Cu(1)-N(3A), 2.010(4); Cu(1)-N(2A), 2.051(5); Cu(1)-Cl(1A), 2.2410(17); Cu(1)-Cl(2A), 2.5281(17); N(1A)-Cu(1)-N(3A), 158.40(19) = α; N(1A)-Cu(1)-N(2A), 80.97(19); N(3A)-Cu(1)-N(2A), 80.23(18); N(1A)-Cu(1)-Cl(1A), 97.29(15); N(3A)-Cu(1)-Cl(1A), 97.99(14); N(2A)-Cu(1)-Cl(1A), 164.56(14) = β; N(1A)-Cu(1)-Cl(2A), 98.08(13); N(3A)-Cu(1)-Cl(2A), 93.50(13); N(2A)-Cu(1)-Cl(2A), 93.17(13); Cl(1A)-Cu(1)-Cl(2A), 102.26(6). For *syn*-[Cu(L^{Ph}OBu)Cl_2]: Cu-N3Ab, 1.970(10); Cu-N(1), 1.981(4); Cu-N3a, 2.012(11); Cu-N(2), 2.077(4); Cu-Cl(1), 2.2771(14) ;Cu-Cl(2), 2.4785(13); N3Ab-Cu-N(1), 162.8(3); N(1)-Cu-N3a, 159.4(3) = β; N3Ab-Cu-N(2), 83.7(3); N(1)-Cu-N(2), 81.61(15); N3a-Cu-N(2), 78.8(3); N3Ab-Cu-Cl(1), 92.8(3); N(1)-Cu-Cl(1),

96.78(11); N3a-Cu-Cl(1), 98.4(4); N(2)-Cu-Cl(1), 154.88(12) = α; N3Ab-Cu-Cl(2), 95.6(3); N(1)-Cu-Cl(2), 96.34(12); N3a-Cu-Cl(2), 93.9(4); N(2)-Cu-Cl(2), 102.83(11); Cl(1)-Cu-Cl(2), 102.27(5). More details are provided as electronic supporting information.

The koneramine formation was unequivocally confirmed while using plethora of metal salts with different anions such as chloride, bromide, nitrate, acetate and perchlorate; anion exchange using silver tosylate did not affect the fragile hemiaminal ether ligand framework (Fig. S10-S14; Table S4; CCDC 1509916, ESI†).

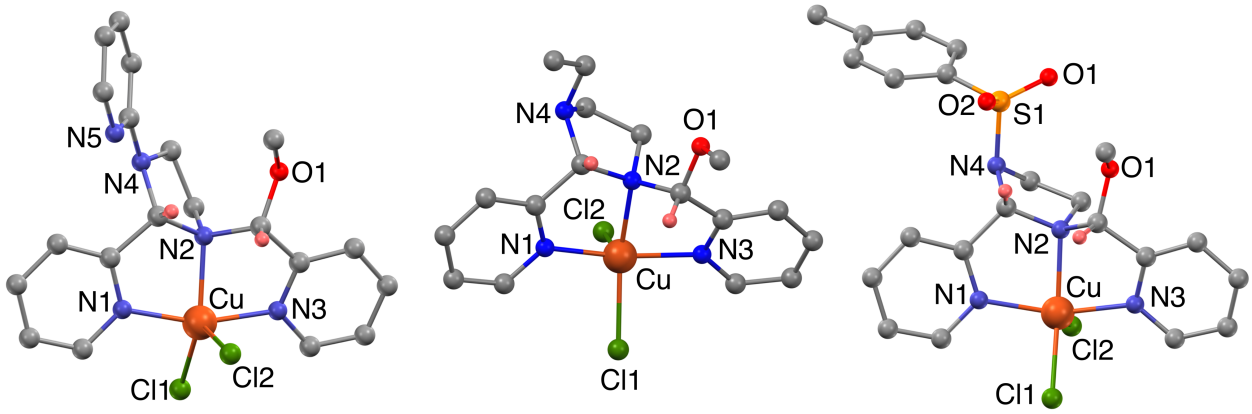

Fig. 4. Solid-state structures of *syn*-[Cu(L^{Py}OMe)Cl_2] (left), *syn*-[Cu(L^{Et}OMe)Cl_2] (middle) and *syn*-[Cu(L^{Ts}OMe)Cl_2] (right). Solvents and H atoms other than those bound to the stereogenic centers are omitted for clarity. Selected bond distances (Å) and angles (°) for *syn*-[Cu(L^{Py}OMe)Cl_2]: Cu-N(1), 1.978(3);Cu-N(3), 1.986(3); Cu-N(2), 2.094(3); Cu-Cl(1), 2.2571(10); Cu-Cl(2), 2.4453(10); N(1)-Cu-N(3), 162.35(11); N(1)-Cu-N(2), 80.38(11); N(3)-Cu-N(2), 81.97(10); N(1)-Cu-Cl(1), 96.85(9); N(3)-Cu-Cl(1), 96.65(8); N(2)-Cu-Cl(1), 140.80(8); N(1)-Cu-Cl(2), 90.35(8); N(3)-Cu-Cl(2), 93.69(8); N(2)-Cu-Cl(2), 102.41(8); Cl(1)-Cu-Cl(2), 116.74(3). For *syn*-[Cu(L^{Et}OMe)Cl_2]: Cu-N(1), 1.987(3); Cu-N(3), 2.007(3); Cu-N(2), 2.110(3); Cu-Cl(1), 2.285(2); Cu-Cl(2), 2.4670(18); N(1)-Cu-N(3), 156.94(13) = β; N(1)-Cu-

N(2), 82.42(13); N(3)-Cu-N(2), 80.71(13); N(1)-Cu-Cl(1), 96.13(10); N(3)-Cu-Cl(1), 92.27(10); N(2)-Cu-Cl(1), 154.15(10) = α; N(1)-Cu-Cl(2), 100.12(11); N(3)-Cu-Cl(2), 99.31(11); N(2)-Cu-Cl(2), 104.77(10); Cl(1)-Cu-Cl(2), 100.90(5). For *syn*-[Cu(L^{Ts}OMe)Cl_2]: Cu-N(1), 1.996(3); Cu-N(3), 2.003(3); Cu-N(2), 2.094(3); Cu-Cl(1), 2.2770(11); Cu-Cl(2), 2.4364(10); N(1)-Cu-N(3), 157.49(13); N(1)-Cu-N(2), 82.40(12); N(3)-Cu-N(2), 80.34(12); N(1)-Cu-Cl(1), 94.56(9); N(3)-Cu-Cl(1), 94.23(9); N(2)-Cu-Cl(1), 152.84(9); N(1)-Cu-Cl(2), 100.99(9); N(3)-Cu-Cl(2), 97.07(9); N(2)-Cu-Cl(2), 103.73(9); Cl(1)-Cu-Cl(2), 103.33(4). More details are provided as electronic supporting information.

We then set out to explore the electronic and steric effects of the *N*-substitution of the ethylenediamine. To this end, we have tried the formation of koneramine complexes using phenyl,[14] ethyl,[14, 15] pyridyl, tosyl and even bulky 1,3,5-triazenyl[17, 20] substituted ethylenediamines (Fig. 4; Fig. S15-S22, ESI†); the koneramine complexes were isolated and characterized in every case. This suggests that the koneramine formation is immune to the size and electronic properties of the *N*-substitution of ethylenediamine component. This allows one to access the koneramine complex with any groups substituted on the non-coordinating backbone nitrogen (N4) such as light-sensitive anthracenyl, pyrenyl or dansyl groups, redox-active ferrocenyl moiety, proton-sensitive pyridyl or pyrazinyl groups and even small molecule binding 1,3,5-triazinyl group.[20]

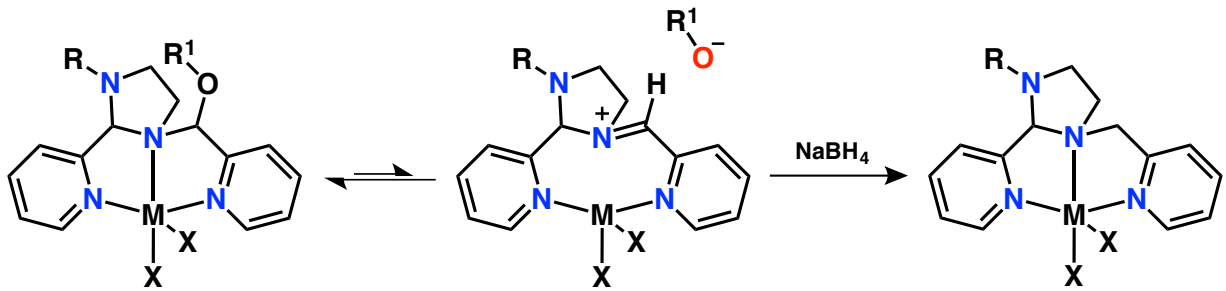

Fig. 5. Postsynthetic modification of coordinated HAE in 1:1 MeOH/$CHCl_3$ mixture at RT.

Even though the koneramine complexes can be assembled in one-pot reactions and they are stable enough to be characterized using multiple analytical techniques, they are fragile in acidic environments and even in protic solvents at times;[20] this is due to the fragile hemiaminal ether linkage that could take part in a dynamic equilibrium with its iminium counterpart, especially in protic and/or nucleophilic solvents (Fig. 5). We took this weak linkage to our advantage by reacting the *syn*-[Cu(L^{Ph}OMe)X_2] complex with $NaBH_4$ directly in a 1:1 solution of MeOH/$CHCl_3$ to obtain the sturdy form of the same complex, *rac*-[Cu(L^{Ph}H)X_2] (observed *m*/*z* for ([Cu(L^{Ph}H)Cl]$^+$ = 414.0660; calculated *m*/*z* = 414.0673; Fig. S23, ESI†). By this single-step postsynthetic modification, a multi-step synthesis of L^{Ph}H was avoided. This PSM was further established unequivocally by using $NaBD_4$ that yielded *rac*-[Cu(L^{Ph}D)X_2], which was confirmed by the ESI-MS envelope corresponding to [Cu(L^{Ph}D)Cl]$^+$ monocation (observed *m*/*z* = 415.0733; calculated *m*/*z* = 415.0735; Fig. S24, ESI†). The solid-state structure of *rac*-[Cu(L^{Ph}H)$(OTs)_2(H_2O)$] was obtained after anion exchange with tosyl anions; the L^{Ph}H is bound to octahedral Cu(II) ion meridionally and the complex is readily soluble in series of solvents including water (Fig. 6; Fig. S25-S27, ESI†).

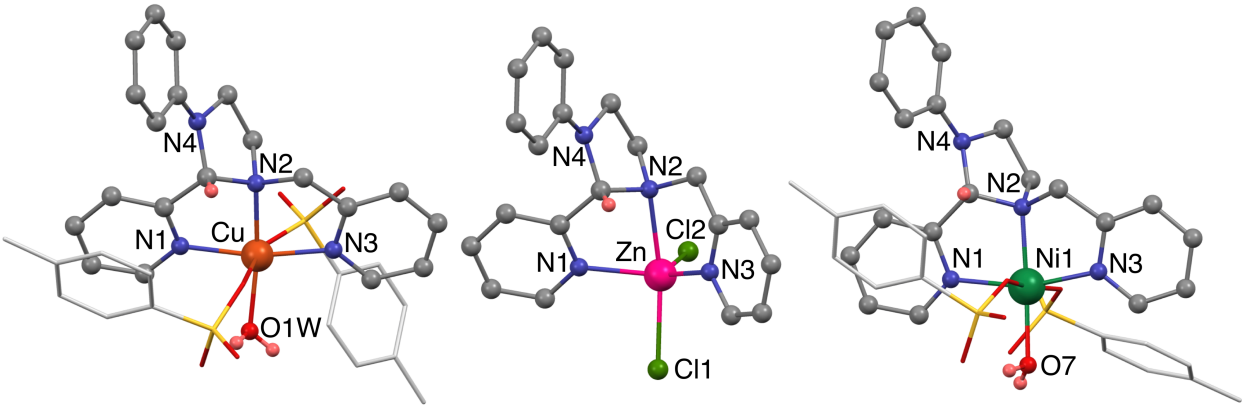

Fig. 6. Solid-state structures of *rac*-[Cu(L^{Ph}H)$(OTs)_2(H_2O)$] (left), *rac*-[Zn(L^{Ph}H)$(Cl)_2$] (middle) and *rac*-[Ni(L^{Ph}H)$(OTs)_2(H_2O)$] (right). Solvents and H atoms other than those bound to

the stereogenic center and of H_2O ligand are omitted for clarity. Selected bond distances (Å) and angles (°) for *rac*-[Cu($L^{Ph}H$)$(OTs)_2(H_2O)$]: Cu-N(3), 1.980(2); Cu-O(1W), 1.988(2); Cu-N(1), 1.990(2); Cu-N(2), 2.019(2); Cu-O(1A), 2.2937(18); Cu-O(1B), 2.6561(18); N(3)-Cu-O(1W), 101.60(9); N(3)-Cu-N(1), 164.44(9); O(1W)-Cu-N(1), 91.56(9); N(3)-Cu-N(2), 83.36(9); O(1W)-Cu-N(2), 166.03(9); N(1)-Cu-N(2), 81.97(9); N(3)-Cu-O(1A), 92.68(8); O(1W)-Cu-O(1A), 86.86(8); N(1)-Cu-O(1A), 96.33(8); N(2)-Cu-O(1A), 106.09(7); N(3)-Cu-O(1B), 90.12(7); O(1W)-Cu-O(1B), 84.54(7); N(1)-Cu-O(1B), 82.84(7); N(2)-Cu-O(1B), 82.38(7); O(1A)-Cu-O(1B), 171.33(6). For), *rac*-[Zn($L^{Ph}H$)$(Cl)_2$]: 2.069(2); Zn-N(3), 2.085(2); Zn-Cl(2), 2.2521(8); Zn-N(2), 2.300(2); Zn-Cl(1), 2.3880(8); N(1)-Zn-N(3), 120.82(9); N(1)-Zn-Cl(2), 111.65(7); N(3)-Zn-Cl(2), 122.50(7); N(1)-Zn-N(2), 76.20(8); N(3)-Zn-N(2), 77.29(9); Cl(2)-Zn-N(2), 94.79(6); N(1)-Zn-Cl(1), 94.27(7); N(3)-Zn-Cl(1), 95.55(7); Cl(2)-Zn-Cl(1), 102.68(3); N(2)-Zn-Cl(1), 162.26(6). For *rac*-[Ni($L^{Ph}H$)$(OTs)_2(H_2O)$]: N(1)-Ni(1), 2.068(3); N(2)-Ni(1), 2.077(3); N(3)-Ni(1), 2.040(3); Ni(1)-O(7), 2.060(3); Ni(1)-O(1), 2.064(2); Ni(1)-O(4), 2.094(2); N(3)-Ni(1)-O(7), 98.40(12); N(3)-Ni(1)-O(1), 85.27(10); O(7)-Ni(1)-O(1), 92.14(12); N(3)-Ni(1)-N(1), 162.97(12); O(7)-Ni(1)-N(1), 97.55(11); O(1)-Ni(1)-N(1), 100.07(11);N(3)-Ni(1)-N(2), 82.10(11); O(7)-Ni(1)-N(2), 175.03(13); O(1)-Ni(1)-N(2), 92.83(11); N(1)-Ni(1)-N(2), 81.50(11); N(3)-Ni(1)-O(4), 83.35(11); O(7)-Ni(1)-O(4), 89.66(12); O(1)-Ni(1)-O(4), 168.62(9); N(1)-Ni(1)-O(4), 90.82(11); N(2)-Ni(1)-O(4), 85.48(10). More details are provided as electronic supporting information.

The sturdy form of the koneramine ligand $L^{Ph}H$ was decoordinated from a dichloromethane solution of [Cu($L^{Ph}H$)Cl_2] by using ammonia solution in good yield and analyzed employing NMR and ESI-MS (Fig. S28-S30, ESI†). The ^{1}H-NMR spectrum of $L^{Ph}H$ is indicative of the newly formed -CH_2 moiety exhibiting key signals for the geminal protons. The ESI-MS of $L^{Ph}H$

shows an envelope corresponding to protonated $L^{Ph}H$ monocation (observed m/z = 317.1760; calculated m/z = 317.1766). Isolated $L^{Ph}H$ is so stable that it can be stored and utilized for prolonged periods. We indeed utilized this $L^{Ph}H$ to make Zn(II) and Ni(II) complexes (Fig. 6; Fig. S31-S38, ESI†). Even though both of *syn*-[Zn($L^{Ph}OMe$)$(Cl)_2$] and *rac*-[Zn($L^{Ph}H$)$(Cl)_2$] possess similar pentacoordinate geometry in their solid-state, in solution they present remarkable difference that is witnessed in their NMR spectra (Fig. 7).

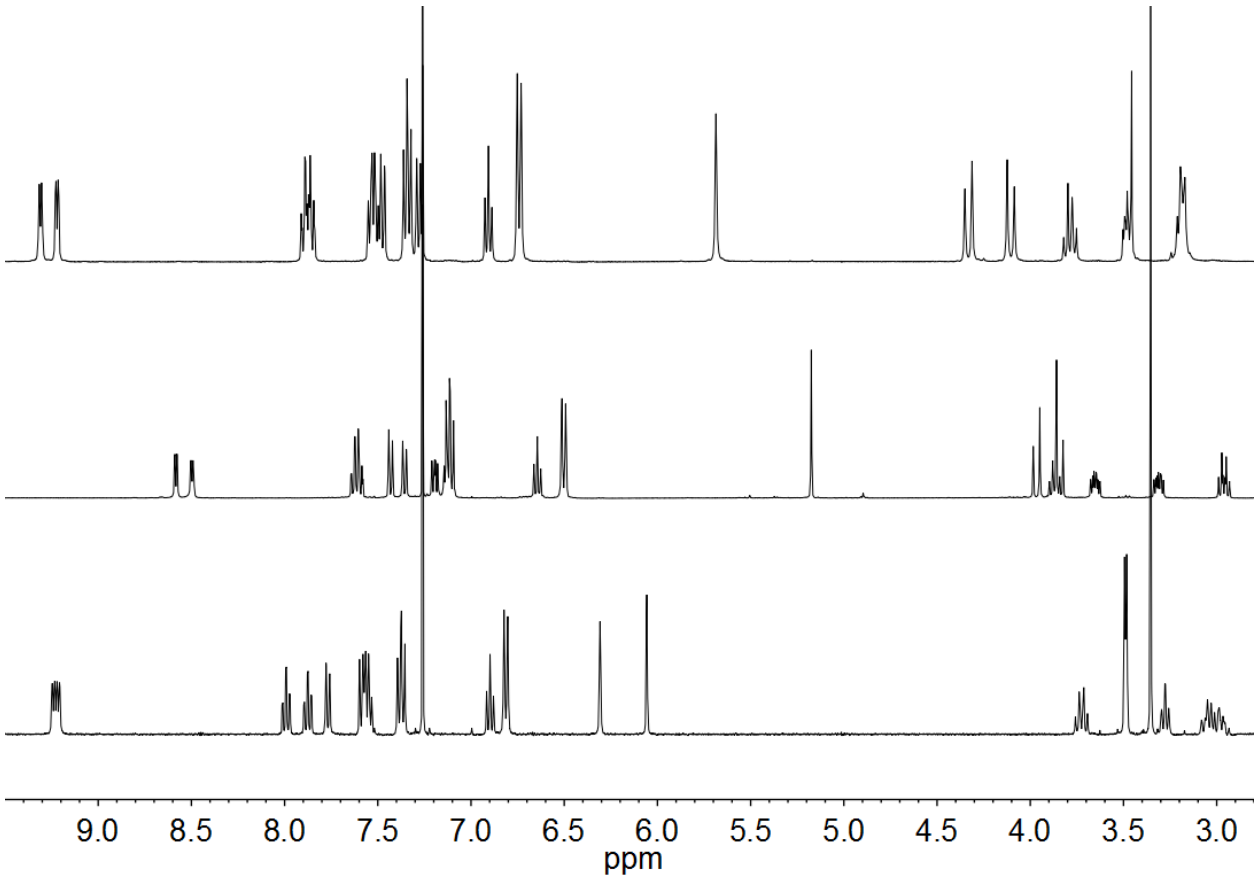

Fig. 7. ^1H NMR spectra of *syn*-[Zn($L^{Ph}OMe$)$(Cl)_2$] (bottom), *rac*-$L^{Ph}H$ decoordinated from *rac*-[Cu($L^{Ph}H$)$(Cl)_2$] (middle) and *rac*-[Zn($L^{Ph}H$)$(Cl)_2$] (top) in $CDCl_3$ at 293 K.

Furthermore, the rigidity of the ligand was further scrutinized with density functional theory calculations using *syn*-[Cu($L^{Ph}OH$)Cl_2] as a model. The optimized structural parameters of *syn*-

[Cu(L^{Ph}OH)Cl_2], *rac*-[Cu(L^{Ph}H)Cl_2] and the proposed iminium intermediate are shown in figure S46. The computed Cu–N and Cu–Cl bond lengths of *syn*-[Cu(L^{Ph}OH)Cl_2][14, 16] and *rac*-[Cu(L^{Ph}H)Cl_2] are in excellent agreement with the X-ray data. Particularly, the axial Cu–N_{tert} bond length in *syn*-[Cu(L^{Ph}OH)Cl_2] is longer and weaker than the other two Cu–N_{tert} bond lengths by ~0.3 Å. The corresponding C–N bond length is ~1.47 Å in *syn*-[Cu(L^{Ph}OH)Cl_2] is prone to be reactive even in the presence of the weak acid. We modeled this reaction by introducing a hydronium ion near the vicinity of *syn*-[Cu(L^{Ph}OH)Cl_2]. During the course of optimization, we note that the OH group abstract a proton from the hydronium ion and detach as water molecule, thus creating an iminium intermediate with a C=N charecter. We note that the Cu–N_{tert} bond is only weakly interacting as indicated from the bond length (2.68 Å). The Lewis basicity of this axial nitrogen is decreased as the negative charge on this center is reduced from –0.30 e^- in *syn*-[Cu(L^{Ph}OMe)Cl_2] to –0.18 e^- in iminium intermediate. In addition, the C–N_{tert} attains a double bond character (C=N_{tert}, 1.33 Å) as shown in figure S46. Finally, a hydride transfer from $NaBH_4$ leads to the formation of *rac*-[Cu(L^{Ph}H)Cl_2] in which the Cu–N_{tert} bond length is reformed with the distance at 2.34 Å and the C–N_{tert} bond length is 1.47 Å. Overall, DFT calculations further support the strengthening of the koneramine to a more rigid framework for the binding of metal ions.

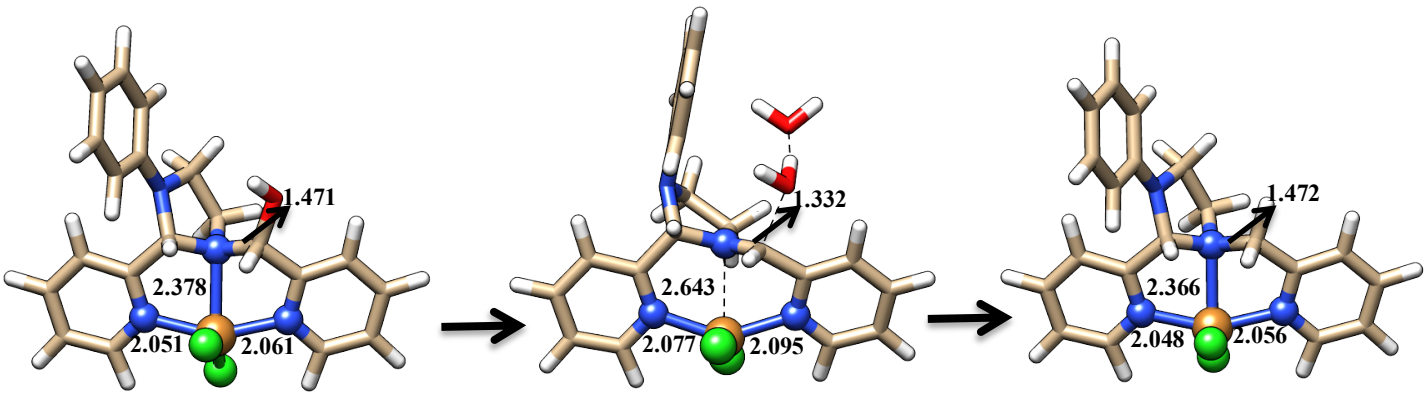

(0.0) **(+9.21)** **(–38.24)**

Fig. 8. DFT

To see if we can resolve the R and S enantiomers of the *rac*-$L^{Ph}H$, hexaaquazinc(II) D-camphor-10-sulfonate was reacted with *rac*-$L^{Ph}H$. The resulted white precipitate showed two sets of signals in the ^{1}H-NMR spectrum as expected (Fig. S39-S42, ESI†).

CONCLUSION. In summary, fragile hemiaminal ether linkages present in the backbone of koneramines (L^ROR') bound to copper(II) in stereoselectively assembled *syn*-[Cu(L^ROR')X_2] complexes have been transformed into sturdy methylene linkages to make corresponding stable *rac*-[Cu(L^RH)Cl_2] complexes by homogeneous postsynthetic modification with the retention of coordination sphere. This work will pave the way for future studies towards simply isolating enantiopure ligands of catalytic importance. Our present efforts are dedicated towards the separation of the enantiopure ligands and complexes.

EXPERIMENTAL SECTION

Materials: Pyridine-2-carboxaldehyde, *N*-ethylethylenediamine, *N*-phenylethylenediamine, $NaBH_4$, $ZnCl_2$, $CuCl_2•2H_2O$, $Cu(NO_3)_2•3H_2O$, $Cu(ClO_4)_2•6H_2O$, $Cu(CH_3COO)_2•H_2O$, $NiCl_2•6H_2O$ and AgOTs were used as received from commercial sources. *Syn*-[Cu($L^{Ph}OMe$)Cl_2][14], *N*^{1}-(pyridine-2-yl)ethane-1,2-diamine[21], *N*-(2-aminoethyl)-4-methylbenzenesulfonamide[22] and Hexaaquazinc(II) D-camphor-10-sulfonate[23] were synthesised as reported. Solvents were distilled under dry nitrogen atmosphere using conventional methods.

Elemental Analyses: Analyses were carried out on a Perkin-Elmer CHNS/O analyser.

NMR Spectroscopy: NMR spectra were recorded on JEOL 500 MHz and JEOL 400 MHz spectrometer. Temperature was kept constant using a variable temperature unit within the error limit of ±1 K. The software MestReNova was used for the processing of the NMR spectra.[24] Tetramethylsilane (TMS) or the deuterated solvent residual peaks were used for calibration.

Mass Spectrometry: Mass spectrometry experiments were performed on a Waters-Q-ToF-Premier-HAB213 equipped with an electrospray interface. Spectra were collected by constant infusion of the sample dissolved in methanol or acetonitrile or dichloromethane with 0.1% formic acid. Mass spectral envelopes were simulated for comparison using freely available software "mMass" an open source mass spectrometry tool.[25]

X-ray crystallography: Single-crystal X-ray data were collected on a Bruker SMART APEX CCD diffractometer using graphite-monochromated Mo Kα radiation (λ = 0.71069 Å). The linear absorption coefficients, the scattering factors for the atoms, and the anomalous dispersion corrections were taken from International Tables for X-ray Crystallography. Data integration and reduction were conducted with SAINT. An empirical absorption correction was applied to the collected reflections with SADABS using XPREP. Structures were determined by direct method using SHELXTL and refined on F^2 by a full-matrix least-squares technique using the SHELXL-97 program package. The lattice parameters and structural data are provided as tables at the end of this Supporting Information. All the structures are deposited in Cambridge Crystallographic Data Centre and the CCDC deposition numbers are provided then and there.

Computational Details: Density functional theory (DFT) calculations are carried out to gain valuable insights on the reactive nature of the chosen *syn*-[Cu(L^{Ph}OEt)Cl_2] complex. Electronic structure calculations are carried out with BP86 functional including Grimme's D3 dispersion

correction with Becke-Johnson damping factor (D3-BJ). All atoms are represented using the *def2*-SV(P) basis set. Analytical vibrational frequencies within the harmonic approximation were computed with the abovementioned basis sets to confirm proper convergence to well-defined minima. Standard approximation was used to obtain zero-point vibrational energy and entropy corrections. We obtained solvation energies using the optimized gas-phase structures from the COSMO solvation model with dielectric constant ε = (methanol) using the default radii. The energies are corrected with the much larger def2-TZVP basis set.

Synthesis:

***Syn*-[Cu(L^{Ph}OEt)Cl$_2$]:[14]** Yield: 68%. Brown colour powder. ESI-MS: *m/z* = 458.0952 (calcd. 458.0935) = $[M\text{-}Cl]^+$. Elemental analysis calculated (%) for $C_{22}H_{24}Cl_2CuN_4O \bullet 0.25CH_2Cl_2$: C, 51.78; H, 4.78; N, 10.86. Found: C, 51.88; H, 4.76; N, 10.70.

***Syn*-[Cu(L^{Ph}OPr)Cl$_2$]:[14]** Yield: 71%. Brown colour powder. ESI-MS: *m/z* = 472.1094 (calcd. 472.1091) = $[M\text{-}Cl]^+$. Elemental analysis calculated (%) for $C_{23}H_{26}Cl_2CuN_4O \bullet 0.15CH_2Cl_2$: C, 53.30; H, 5.08; N, 10.74. Found: C, 53.25; H, 5.0; N, 10.66.

***Syn*-[Cu(L^{Ph}OBu)Cl$_2$]:[14]** Yield: 57%. Parrot green colour powder. ESI-MS: *m/z* = 486.1248 (calcd. 486.1240) = $[M\text{-}Cl]^+$. Elemental analysis calculated (%) for $C_{24}H_{28}Cl_2CuN_4O \bullet 0.1CH_2Cl_2$: C, 54.47; H, 5.35; N, 10.54. Found: C, 54.58; H, 5.23; N, 10.25.

***Syn*-[Cu(L^{Ph}OMe)(NO$_3$)$_2$].[14]** $[M\text{-}2(NO_3)]^+ = C_{21}H_{22}CuN_4O$ = 409.1090 (calcd); 409.1104 (obs). $[M\text{-}2(NO_3)+Cl]^+ = C_{21}H_{22}CuN_4OCl$ = 444.0778 (calcd); 444.0786 (obs). $[M\text{-}2(NO_3)+HCOO]^+ = C_{22}H_{23}CuN_4O_3$ = 454.1066 (calcd); 454.1071 (obs). The Cl^- and $HCOO^-$ must have originated from the chlorinated solvents and formic acid used to infuse the sample

while measurement. Complete details on the synthesis, single crystal X-ray structure and ESI-MS characterisations of *syn*-[Cu(L^{Ph}OMe)Cl_2] including simulated mass envelopes have been provided in a recent report.

***Syn*-[Cu(L^{Ph}OMe)$(OAc)_2$].[14]** [M-2(OAc)]$^+$ = $C_{21}H_{22}CuN_4O$ = 409.1090 (calcd); 409.1099 (obs). [M-2(OAc)+Cl]$^+$ = $C_{21}H_{22}CuN_4OCl$ = 444.0778 (calcd); 444.0789 (obs). [M-2(OAc)+HCOO]$^+$ = $C_{22}H_{23}CuN_4O_3$ = 454.1066 (calcd); 454.1077 (obs).

***Syn*-[Cu(L^{Ph}OMe)$(ClO_4)_2$].[14]** [M-2(ClO_4)]$^+$ = $C_{21}H_{22}CuN_4O$ = 409.1090 (calcd); 409.1084 (obs). [M-2(ClO_4)+Cl]$^+$ = $C_{21}H_{22}CuN_4OCl$ = 444.0778 (calcd); 444.0775 (obs). [M-2(ClO_4)+HCOO]$^+$ = $C_{22}H_{23}CuN_4O_3$ = 454.1066 (calcd); 454.1049 (obs).

***Syn*-[Cu(L^{Et}OMe)Cl_2]:** In a 100 ml round bottom flask, pyridine-2-carboxaldehyde (1.071 g, 10 mmol) was dissolved in 20 ml methanol by stirring for 5 min. Methanolic solution (20 ml) of *N*-ethylethylenediamine (0.4408 g, 5 mmol) was added drop-wise into the stirred aldehyde solution. The yellow mixture was left to stir at room temperature for 24 h. Methanolic solution (5 ml) of $CuCl_2$•$2H_2O$ (0.851 g, 5 mmol) was added drop-wise into the solution of hemiaminalether, **L^{Et}OMe**. A bottle green precipitate started to appear within 15 minutes after adding the solution of metal salt. The reaction mixture was left to stir for 3 h at room temperature. The green precipitate was filtered off and recrystallized in methanol. The green filtrate left at 0 °C for one day forms bottle green crystals were suitable for SCXRD. Yield: 1.1 g (51%). ESI-MS: *m/z* = 396.0783 (calcd. 396.0778) = [M-Cl]$^+$. Elemental analysis calculated (%) for $C_{17}H_{22}Cl_2CuN_4O$: C, 47.17; H, 5.12; N, 12.94. Found: C, 47.22; H, 5.07; N, 12.83.

***Syn*-[Cu(L^{Et}OMe)$(NO_3)_2$].[14]**

Yield: 68%. Bottle green powder. $[M\text{-}2(NO_3)+Cl]^+ = C_{17}H_{22}CuN_4OCl$ = 396.0778 (calcd); 396.0789 (obs). $[M\text{-}2(NO_3)+HCOO]^+ = C_{18}H_{23}CuN_4O_3$ = 406.1066 (calcd); 406.1053 (obs). $[M\text{-}2(NO_3)+CH_3COO]^+ = C_{19}H_{25}CuN_4O_3$ = 420.1233 (calcd); 406.1221 (obs). The Cl^-, $HCOO^-$ and CH_3COO^-, must have originated from the chlorinated solvents and formic acid used to infuse the sample while measurement.

***Syn*-[Cu(L^{Ts}OMe)Cl_2]:** In a 50 ml round bottom flask, pyridine-2-carboxaldehyde (0.107 g, 1 mmol) was dissolved in 3 ml methanol by stirring for 5 min. Methanolic solution (5 ml) of *N*-(2-aminoethyl)-4-methylbenzenesulfonamide (0.105 g, 0.5 mmol) was added drop-wise into the stirred aldehyde solution. The yellow mixture was left to stir at room temperature for 24 h. Methanolic solution (2 ml) of $CuCl_2•2H_2O$ (85 mg, 0.5 mmol) was added drop-wise into the solution of hemiaminalether, **L^{Ts}OMe**. A bottle green precipitate started to appear within 30 minutes of adding the solution of metal salt. The reaction mixture was left to stir for 3 h at room temperature. The greenish blue precipitate was filtered off and the blue filtrate left at 0 °C for a week forms blue crystals were suitable for SCXRD. Yield: 0.135 g (48%). ESI-MS: *m*/*z* =522.0601 (calcd. 522.0554) = $[M\text{-}Cl]^+$. Elemental analysis calculated (%) for $C_{22}H_{24}Cl_2CuN_4O_3S•0.5Et_2O$: C, 48.36; H, 4.90; N, 9.40. Found: C, 48.10; H, 4.70; N, 9.48.

***Syn*-[Cu(L^{Py}OMe)Cl_2]:** In a 50 ml round bottom flask, pyridine-2-carboxaldehyde (0.107 g, 1 mmol) was dissolved in 3 ml methanol by stirring for 5 min. Methanolic solution (5 ml) of N^1-(pyridine-2-yl)ethane-1,2-diamine (69 mg, 0.5 mmol) was added drop-wise into the stirred aldehyde solution. The yellow mixture was left to stir at room temperature for 24 h. Methanolic solution (2 ml) of $CuCl_2•2H_2O$ (85 mg, 0.5 mmol) was added drop-wise into the solution of hemiaminalether, **L^{Py}OMe**. A green precipitate started to appear within 30 minutes of adding the solution of metal salt. The reaction mixture was left to stir for 12 h at room

temperature. The green precipitate was filtered off and recrystallized in methanol (20 ml). The green filtrate left at 0 °C for a day forms green crystals were suitable for SCXRD. Yield: 0.142 g (61%). ESI-MS: *m/z* =.445.0734. (calcd. 445.0731) = $[M\text{-}Cl]^+$. Elemental analysis calculated (%) for $C_{20}H_{21}Cl_2CuN_5O$ $0.5CH_3OH$ $0.2CH_2Cl_2$: C, 48.29; H, 4.52; N, 13.60. Found: C, 48.32; H, 4.54; N, 13.067.

Post synthetic modification of *Syn*-[Cu(L^{Ph}OMe)Cl_2] to [Cu(L^{Ph}H)Cl_2]: In a 100 ml Schlenk flask, *syn*-[Cu(L^{Ph}OMe)Cl_2] (0.481 g, 1 mmol) was dissolved in 1:1 methanol/chloroform mixture (50 ml) and $NaBH_4$ (0.378 g, 10 mmol) was added all at once. This mixture was stirred at room temperature under N_2 atmosphere for 20 h and then in open air for an hour. All the volatiles were evaporated to get a green residue, which was dissolved in 20 ml dichloromethane and brine (20 ml) was added to this solution. After stirring for three hours, the organic layer was separated, washed with brine (2 × 20 ml), dried with $MgSO_4$, evaporated to get a dark green precipitate (0.279 g, 62%). ESI-MS: *m/z* = 414.0660 (calcd 414.0673). Elemental analysis calculated (%) for $C_{20}H_{20}Cl_2N_4Cu{\cdot}0.5CH_2Cl_2{\cdot}0.4Et_2O$: C, 50.76; H, 4.82; N, 10.71. Found: C, 50.91; H, 4.76; N, 10.83.

[Cu(L^{Ph}H)$(OTs)_2(H_2O)$]: [Cu(L^{Ph}H)Cl_2] was dissolved in acetonitrile, two equivalents of AgOTs was added and the resulting solution was stirred for an hour in dark at room temperature. The mixture was filtered thru Celite and the filtrate was evaporated to dryness to obtain [Cu(L^{Ph}H)$(OTs)_2(H_2O)$] as green powder. Crystals suitable for X-ray diffraction were obtained within a day from an acetonitrile solution kept at 0 °C. ESI-MS: *m/z* = 550.1105 (calcd 550.1100) = $[M\text{-}(OTs+H_2O)]^+$; m/z = 424.0948 (calcd 424.0961) =$[M\text{-}(2OTs+H_2O)+HCOO]^+$.

Elemental analysis calculated (%) for $C_{34}H_{36}N_4O_7S_2Cu \cdot 0.5H_2O$: C, 54.50; H, 4.98; N, 7.48. Found: C, 54.39; H, 4.68; N, 7.43.

Isolation of $L^{Ph}H$ from $[Cu(L^{Ph}H)Cl_2]$:[26] In a 50 ml round bottom flask, $[Cu(L^{Ph}H)Cl_2]$ (0.451 g, 1 mmol) was dissolved in 15 ml dichloromethane, 6 ml ammonium hydroxide solution (28-30% NH_3 basis) was added and stirred for 1 h at room temperature. The pale yellow organic layer was separated from the blue aqueous layer, washed with brine (2 × 10 ml), dried using $MgSO_4$ and evaporated the solvent to obtain the $L^{Ph}H$ as pale yellow oil. Yield: 0.196 g (62%). ^{1}H NMR (400.16 MHz, 25 °C, $CDCl_3$): δ = 8.59 (d, 1H, Py), 8.50 (d, 1H, Py), 7.64 (d, 1H, Py), 7.60 (d, 1H, Py), 7.44 (d, 1H, Py), 7.37 (d, 1H, Py), 7.21 (m, 1H, Py), 7.12 (m, 3H, Py and Ph), 6.64 (t, 1H, Ph), 6.50 (d, 2H, Ph), 5.17 (s, 1H, C*H), 3.98-3.82 (m, 3H, CH_2-Py and 1H-Im), 3.66 (m, 1H, Im), 3.31 (m, 1H, Im), 2.96 (m, 1H, Im). ^{13}C NMR (100 MHz, 25 °C, $CDCl_3$): δ = 161.20 (Ar), 158.79 (Ar), 149.15 (Ar), 148.86 (Ar), 146.12 (Ar), 137.01 (Ar), 136.56 (Ar), 129.11 (Ar), 123.23 (Ar), 123.13 (Ar), 122.29 (Ar), 122.18 (Ar), 116.84 (Ar), 112.71 (Ar), 83.13 (CH), 58.42 (CH_2-Py), 50.77 (CH_2, Im), 47.90 (CH_2, Im). ESI-MS: *m/z* = 317.1760 (calcd 317.1766) = $[M+H]^+$.

$[Zn(L^{Ph}H)Cl_2]$: In a 50 ml round bottom flask was charged with $L^{Ph}H$ (95 mg, 0.3 mmol) in 20 ml methanol and anhydrous $ZnCl_2$ (41 mg, 0.3 mmol) was added as a methanolic solution (5 ml). The resulting solution was heated at 60 °C for three hours, then the solution was concentrated to 5 ml, ether was added (20 ml) to obtain white precipitate of $[Zn(L^{Ph}H)Cl_2]$ in 72% yield (98 mg).^{1}H NMR (400.16 MHz, 25 °C, $CDCl_3$): δ = 9.31 (d, 1H, Py), 9.22 (d, 1H, Py), 7.87 (m, 2H, Py), 7.51 (m, 3H, Py), 7.34 (t, 2H, Ph), 7.28 (d, 1H, Py), 6.91 (t, 1H, Ph), 6.75 (d, 2H, Ph), 5.69 (s, 1H, C*H), 4.35-4.09 (dd, 2H, CH_2-Py), 3.79 (m, 1H, Im), 3.49 (m, 2H, Im), 3.19 (m, 1H, Im).

^{13}C NMR (100 MHz, 25 °C, $CDCl_3$): δ = 155.17 (Ar), 153.08 (Ar), 150.00 (Ar), 149.73 (Ar), 146.70 (Ar), 140.22 (Ar), 140.04 (Ar), 130.14 (Ar), 125.35 (Ar), 124.96 (Ar), 123.63 (Ar), 123.27 (Ar), 118.90 (Ar), 111.82 (Ar), 80.98 (CH), 56.77 (CH_2-Py), 51.15 (CH_2, Im), 44.34 (CH_2, Im). ESI-MS: m/z = 415.0679 (calcd 415.0668) = $[M\text{-}Cl]^+$; *m/z* = 425.0963 (calcd 425.0956). Elemental analysis calculated (%) for $C_{20}H_{20}Cl_2N_4Zn{\cdot}0.3H_2O{\cdot}0.3CHCl_3$: C, 49.36; H, 4.26; N, 11.34. Found: C, 49.38; H, 4.12; N, 11.42.

[Ni($L^{Ph}H$)Cl_2]: In a 50 ml round bottom flask was charged with $L^{Ph}H$ (95 mg, 0.3 mmol) in 20 ml methanol and anhydrous $NiCl_2{\bullet}6H_2O$ (71 mg, 0.3 mmol) was added as a methanolic solution (5 ml). The resulting solution was heated at 60 °C for three hours, then the solution was concentrated to 5 ml, ether was added (20 ml) to obtain turquoise green precipitate of [Ni($L^{Ph}H$)Cl_2] in 80% yield (0.107 g). ESI-MS: *m/z* = 409.0757 (calcd 409.0730) = $[M\text{-}Cl]^+$. Elemental analysis calculated (%) for $C_{20}H_{20}Cl_2N_4Ni{\cdot}0.6H_2O{\cdot}0.2CH_3CN$: C, 52.69; H, 4.73; N, 12.65. Found: C, 52.85; H, 4.36; N, 12.49.

[Ni($L^{Ph}H$)(H_2O)($OTs)_2$]: [Ni($L^{Ph}H$)Cl_2] was dissolved in acetonitrile, two equivalents of AgOTs was added and the resulting solution was stirred for an hour in dark at room temperature. The mixture was filtered thru Celite and the filtrate was evaporated to dryness to obtain [Ni($L^{Ph}H$)(H_2O)($OTs)_2$] as greenish blue powder. Crystals suitable for X-ray diffraction were obtained within a day from an acetonitrile solution kept at 0 °C. ESI-MS: *m/z* = 545.1158 (calcd 545.1157) = $[M\text{-}(OTs+H_2O)]^+$; m/z = 419.1008 (calcd 419.1018) =$[M\text{-}(2OTs+H_2O)+HCOO]^+$. Elemental analysis calculated (%) for $C_{34}H_{36}N_4O_7S_2Ni{\cdot}0.3H_2O$: C, 55.12; H, 4.98; N, 7.56. Found: C, 55.01; H, 4.89; N, 7.47.

[Zn(L^{Ph}H)(D-CS)$_2$]: In a 50 ml round bottom flask was charged with L^{Ph}H (32 mg, 0.1 mmol) in 10 ml methanol and anhydrous hexaaquazinc(II) D-camphor-10-sulfonate (63 mg, 0.1 mmol) was added as a methanolic solution (5 ml). The resulting solution was heated at 70 °C for 2 h, then the solution was concentrated to 2 ml, ether was added (20 ml) to obtain white precipitate of [Zn(L^{Ph}H)(D-CS)$_2$]. Yield = 65 mg (77 %). ^{1}H NMR (400.16 MHz, 25 °C, $CDCl_3$) δ = 9.10 – 8.96 (m, 2H, Py), 7.92 – 7.84 (m, 1H, Py), 7.60 – 7.49 (m, 4H, Py and Ph), 7.38-7.33 (m, 2H, Py), 7.29-7.26 (m, 1H, Py), 6.93 – 6.86 (m, 1H, Ph), 6.82 (d, *J* = 8.1 Hz, 2H, Ph), 5.98 (d, *J* = 30.7 Hz, 1H, C*H), 4.54-4.51 (m, 1H, CH_2-Py), 4.11 (dd, *J* = 15.3, 10.7 Hz, 1H, CH_2-Py), 3.79-3.72 (m, 1H, Im-CH_2), 3.52-3.47 (m, 1H, Im-CH_2), 3.42 – 3.20 (m, 3H, Im-CH_2), 3.17 (d, *J* = 14.7 Hz, 2H, CS), 2.70 (d, *J* = 14.8 Hz, 2H, CS), 2.57 – 2.47 (m, 2H, CS), 2.26 (d, *J* = 18.3 Hz, 2H, CS), 1.99 (t, *J* = 4.4 Hz, 1H, Im-CH_2), 1.96 – 1.88 (m, 2H, CS), 1.75 (d, *J* = 18.3 Hz, 2H), 1.49-1.42 (m, 4H, CS), 1.29-1.22 (m, 4H, CS), 1.01 (s, 6H, CH_3-CS), 0.75 (s, 6H, CH_3-CS). ^{13}C NMR (100 MHz, 25 °C, $CDCl_3$): δ = 216.58 (CS), 156.15 (Ar), 155.89 (Ar), 153.79 (Ar), 148.83 (Ar), 148.43 (Ar), 148.27 (Ar), 146.88 (Ar), 146.80 (Ar), 140.18 (Ar), 140.03 (Ar), 139.86 (Ar), 129.94 (Ar), 125.14 (Ar), 124.93 (Ar), 124.75 (Ar), 123.59 (Ar), 118.61 (Ar), 112.10 (Ar), 81.95 (C*H), 58.31 CS), 57.20(CH_2-Py), 50.66 (CS), 47.87(Im-CH_2), 47.25 (CS), 44.60 (Im-CH_2), 42.80 (CS), 42.56 (CS), 26.94 (CS), 24.48 (CS), 19.87 (CS), 19.77 (CS). ESI-MS: *m*/*z* = 611.1682 (calcd 611.1670) = [Zn(L^{Ph}H)(CS)]$^+$; *m*/*z* = 425.0921 (calcd 425.0956) = [Zn(L^{Ph}H)HCOO]$^+$. Elemental analysis calculated (%) for $C_{40}H_{50}N_4O_8S_2Zn{\cdot}0.5H_2O$: C,56.30; H, 6.02; N, 6.57. Found: C, 56.38; H, 6.11; N, 6.61.

ASSOCIATED CONTENT

Supporting Information. The Supporting Information is available free of charge on the ACS Publications website at DOI: 10.1021/

^{1}H NMR, electrospray mass ionisation spectra, single crystal X-ray diffraction data, packing diagrams, crystallographic details and DFT details (PDF)

Accession Codes.

CCDC 1509913-1509923 contain the supplementary crystallographic data for this paper. These data can be obtained free of charge via www.ccdc.cam.ac.uk/data_request/cif, or by emailing data_request@ccdc.cam.ac.uk, or by contacting The Cambridge Crystallographic Data Centre, 12 Union Road, Cambridge CB2 1EZ, UK; fax: +44 1223 336033.

Corresponding Author

Raja Angamuthu - Department of Chemistry, Indian Institute of Technology Kanpur, Kanpur 208016, India; Department of Sustainable Energy Engineering, Indian Institute of Technology Kanpur, Kanpur 208016, India; orcid.org/0000-0002-5152-0837; E-mail: raja@iitk.ac.in

Authors

Sakthi Raje - Department of Chemistry, Indian Institute of Technology Kanpur, Kanpur 208016, India; orcid.org/ 0000-0001-6825-3942; E-mail: sakthir@iitk.ac.in

Mahesh Sundararajan - Theoretical Chemistry Section, Chemistry Division, Bhabha Atomic Research Centre, Mumbai-400085, India; Homi Bhabha National Institute, Mumbai – 400 085, India; orcid.org/0000-0002-1522-124X; E-mail: smahesh@barc.gov.in

Notes

The authors declare no competing financial interest.

Author Contributions

RA designed the work. SR executed the experiments. MS performed the DFT studies. RA and SR wrote the paper.

ACKNOWLEDGMENT

SR and RA acknowledge the Council of Scientific and Industrial Research for the Senior Research Fellowship and the Science and Engineering Research Board for the financial support (EMR/2015/001350 and CRG/2020/001708), respectively. Abhishek Koner is gratefully acknowledged for the preliminary studies.

REFERENCES

(1) Zheng, W.; Chen, L. J.; Yang, G.; Sun, B.; Wang, X.; Jiang, B.; Yin, G. Q.; Zhang, L.; Li, X. P.; Liu, M. H.; Chen, G. S.; Yang, H. B., Construction of Smart Supramolecular Polymeric Hydrogels Cross linked by Discrete Organoplatinum(II) Metallacycles via Post Assembly Polymerization. *J. Am. Chem. Soc.* **2016,** *138*, 4927-4937.

(2) Brega, V.; Zeller, M.; He, Y.; Peter Lu, H.; Klosterman, J. K., Multi-responsive metal-organic lantern cages in solution. *Chem. Commun. (Cambridge, U. K.)* **2015,** *51*, 5077-5080.

(3) Beves, J. E.; Danon, J. J.; Leigh, D. A.; Lemonnier, J. F.; Vitorica-Yrezabal, I. J., A Solomon Link through an Interwoven Molecular Grid. *Angew. Chem., Int. Ed.* **2015,** *54*, 7555-7559.

(4) Schneider, M. W.; Oppel, I. M.; Griffin, A.; Mastalerz, M., Post-Modification of the Interior of Porous Shape-Persistent Organic Cage Compounds. *Angew. Chem. Int. Ed.* **2013,** *52*, 3611-3615.

(5) Zhao, D.; Tan, S.; Yuan, D.; Lu, W.; Rezenom, Y. H.; Jiang, H.; Wang, L.-Q.; Zhou, H.-C., Surface Functionalization of Porous Coordination Nanocages Via Click Chemistry and Their Application in Drug Delivery. *Adv. Mater.* **2011,** *23*, 90-93.

(6) Roberts, D. A.; Castilla, A. M.; Ronson, T. K.; Nitschke, J. R., Post-assembly Modification of Kinetically Metastable FeII2L3 Triple Helicates. *J. Am. Chem. Soc.* **2014,** *136*, 8201-8204.

(7) Burrows, A. D.; Cohen, S. M., Postsynthetic modification of coordination networks. *CrystEngComm* **2012,** *14*, 4095-4095.

(8) Belowich, M. E.; Stoddart, J. F., Dynamic imine chemistry. *Chem. Soc. Rev.* **2012,** *41*, 2003-2024.

(9) Corbett, P. T.; Leclaire, J.; Vial, L.; West, K. R.; Wietor, J.-L.; Sanders, J. K. M.; Otto, S., Dynamic Combinatorial Chemistry. *Chem. Rev.* **2006,** *106*, 3652-3711.
(10) Sarma, R. J.; Nitschke, J. R., Self-assembly in systems of subcomponents: simple rules, subtle consequences. *Angew. Chem., Int. Ed.* **2008,** *47*, 377-380.
(11) Young, M. C.; Johnson, A. M.; Hooley, R. J., Self-promoted post-synthetic modification of metal-ligand M2L3 mesocates. *Chem. Commun. (Cambridge, U. K.)* **2014,** *50*, 1378-1380.
(12) Waller, P. J.; Lyle, S. J.; Osborn Popp, T. M.; Diercks, C. S.; Reimer, J. A.; Yaghi, O. M., Chemical Conversion of Linkages in Covalent Organic Frameworks. *J Am Chem Soc* **2016,** *138*, 15519-15522.
(13) Li, H.; Yao, Z.-J.; Liu, D.; Jin, G.-X., Multi-component coordination-driven self-assembly toward heterometallic macrocycles and cages. *Coord. Chem. Rev.* **2015,** *293-294*, 139-157.
(14) Raje, S.; Gurusamy, S.; Koner, A.; Mehrotra, S.; Jennifer, S. J.; Vasudev, P. G.; Butcher, R. J.; Angamuthu, R., Multicomponent One-pot Reactions Towards the Synthesis of Stereoisomers of Dipicolylamine Complexes. *Chem. Asian. J.* **2016,** *11*, 128-135.
(15) Raje, S.; Mani, K.; M. Parsutkar, M.; Angamuthu, R., Metal Ions as External Stimuli in Stereoselective Self-Sorting of Koneramines and Thiokoneramines. *New J. Chem.* **2017,** *41*, 12303-12308.
(16) Raje, S.; Mondivagu, N.; Chahal, M.; Butcher Ray, J.; Angamuthu, R., Mechanism of Evolution of Koneramine Complexes from One-Pot Reactions: Snapshots of Intermediates Offer Facile Routes to New Dipicolylamines. *Chem. Asian. J.* **2018,** *13*, 1458-1466.
(17) Mehrotra, S.; Raje, S.; Jain, A. K.; Jain, A.; Kandasamy, P.; Butcher, R. J.; Angamuthu, R., A Quest towards Eccentric Piedfort Pairs. *ChemistrySelect* **2018,** *3*, 4844-4850.
(18) Lal, B.; Gund, V. G., Approaches towards the stabilization of hemiaminal function at ornithine unit of mulundocandin. *Bioorganic & Medicinal Chemistry Letters* **2004,** *14*, 1123-1128.
(19) Wu, Y.-C.; Bernadat, G.; Masson, G.; Couturier, C.; Schlama, T.; Zhu, J., Synthetic Studies on (-)-Lemonomycin: An Efficient Asymmetric Synthesis of Lemonomycinone Amide. *J. Org. Chem.* **2009,** *74*, 2046-2052.
(20) Chahal, M.; Raje, S.; Kotana, G.; Angamuthu, R., Binding enabled catalytic activation of SO_2 by copper koneramine complexes under ambient conditions. *Green Chem.* **2019,** *21*, 6372-6380.
(21) Robinson, A.; Thomas, G. L.; Spandl, R. J.; Welch, M.; Spring, D. R., Gemmacin B: bringing diversity back into focus. *Org. Biomol. Chem.* **2008,** *6*, 2978-2981.
(22) St John-Campbell, S.; White, A. J. P.; Bull, J. A., Single operation palladium catalysed C(sp3)-H functionalisation of tertiary aldehydes: investigations into transient imine directing groups. *Chem. Sci.* **2017,** *8*, 4840-4847.
(23) Schepke, M.; Edelmann, F. T.; Blaurock, S., Hexaaquazinc(II) D-camphor-10-sulfonate. *Acta Crystallogr., Sect. E: Struct. Rep. Online* **2007,** *63*, m2071.
(24) Willcott, M. R., MestRe Nova. *J. Am. Chem. Soc.* **2009,** *131*, 13180-13180.

(25) Strohalm, M.; Kavan, D.; Novak, P.; Volny, M.; Havlicek, V., mMass 3: A Cross-Platform Software Environment for Precise Analysis of Mass Spectrometric Data. *Anal. Chem.* **2010,** *82*, 4648-4651.
(26) Itoh, S.; Taki, M.; Nakao, H.; Holland, P. L.; Tolman, W. B.; Que, L.; Fukuzumi, S., Aliphatic hydroxylation by a bis(mu-oxo)dicopper(III) complex. *Angew. Chem. Int. Ed.* **2000,** *39*, 398-400.